

Determination of Ionic Diffusion Coefficients in Ion-Exchange Membranes: Strong Electrolytes and Sulfates with Dissociation Equilibria

Kuldeep,^[a] José A. Manzanares,^[b] Pertti Kauranen,^[c] Seyedabolfazl Mousaviihashemi,^[a] and Lasse Murtomäki*^[a]

An Invited Contribution to the Hubert Girault Festschrift.

Ionic diffusion coefficients in the membrane are needed for the modelling of ion transport in ion-exchange membranes (IEMs) with the Nernst-Planck equation. We have determined the ionic diffusion coefficients of Na^+ , OH^- , H^+ , Cl^- , SO_4^{2-} , NaSO_4^- , and HSO_4^- from the diffusion experiments of dilute NaCl , NaOH , HCl , Na_2SO_4 , and H_2SO_4 solutions through IEMs and the membrane conductivity measured in these solutions, using electrochemical impedance spectroscopy. The order of diffusion fluxes across the anion-exchange membrane is found to be as $\text{H}_2\text{SO}_4 > \text{HCl} > \text{NaCl} > \text{Na}_2\text{SO}_4 > \text{NaOH}$, whereas for the cation-exchange membrane it was $\text{NaOH} > \text{NaCl} > \text{Na}_2\text{SO}_4 \geq \text{H}_2\text{SO}_4$. Special attention is given to sulfates because of the partial

dissociation of bisulfate and NaSO_4^- , which makes the use of the Nernst-Hartley equation, that is, splitting the electrolyte diffusion coefficient into its ionic contributions, impossible. The expression of the diffusion coefficient of sulfates taking into account the dissociation equilibrium has been derived and the corresponding Fick equation has been integrated. In addition, for sulfates, finite element simulations with COMSOL Multiphysics, applying a homogeneous membrane model, were done to give estimates of their ionic diffusion coefficients. This work offers a convenient approach to finding diffusion coefficients of various ions inside IEMs.

Introduction

Membrane separation processes are employed in the research and applications of various wastewater treatment processes. Examples of such include the usage of bipolar electro dialysis to treat sodium sulfate stemming from the growing lithium-ion battery industry,^[1] reverse electro dialysis,^[2] membrane-assisted capacitive deionization,^[3] desalination and chemical recovery applications,^[1,4] water electrolysis,^[5] water-splitting in photoelectrochemical cells,^[6] and fuel cells.^[7-9]

A detailed theoretical study of ion transport inside the membrane has already been published in various articles and

books.^[10-12] Furthermore, a number of experimental techniques, e.g., ion-exchange measurements,^[13-16] conductivity,^[17-21] radio-labeled diffusion,^[22-24] and Donnan dialysis^[25] have also been used to measure the diffusion coefficients in IEMs.^[26-28] All of these methods are applicable only for binary strong electrolytes. Modern techniques like NMR spectrometer diffusive units can also measure self-diffusion coefficients for NMR active nuclei.^[29] None of these methods are suitable to measure the diffusion coefficients of ions of weak electrolytes.


Electrochemical impedance spectroscopy (EIS) can be used to determine the properties of an electrochemical system, and complex mathematical expressions are often needed to explain the impedance. The most straightforward application of EIS is to determine the ohmic resistance of a system. When studying membranes, EIS has been used to find out membrane conditions,^[30] conductivity,^[31] transfer kinetics,^[32] and fouling and scaling.^[33,34] Nikonenko^[32] et al. developed an equivalent circuit for the impedance of an ion-exchange membrane (IEM), assuming that all ions had the same diffusion coefficients in the aqueous and membrane phases.


In our previous paper,^[35] we reported studies of electrodiffusion across IEMs. Ionic diffusion coefficients were taken as 10% of their values in aqueous solutions at infinite dilution, except for H^+ for which it was 60% of its aqueous value. These values were chosen to fit experimental fluxes to Finite Element Method (FEM) simulations with COMSOL Multiphysics®. To justify that choice, in this work we determine ionic diffusion coefficients in IEMs by combining membrane resistance measurements with EIS and diffusion experiments of various strong electrolytes. With partially dissociating electrolytes, H_2SO_4 and

[a] Kuldeep, Dr. S. Mousaviihashemi, Prof. L. Murtomäki
Department of Chemistry and Materials Science, School of Chemical Engineering
Aalto University
PO Box 1600, 00076 AALTO, Finland
E-mail: lasse.murtomaki@aalto.fi

[b] Prof. J. A. Manzanares
Department of Thermodynamics
University of Valencia
c/Dr. Moliner, 50. E-46100 Burjassot, Spain

[c] Prof. P. Kauranen
LUT University
School of Energy Systems
P.O. Box 20, 53851 Lappeenranta, Finland

 Supporting information for this article is available on the WWW under <https://doi.org/10.1002/celec.202200403>

 © 2022 The Authors. ChemElectroChem published by Wiley-VCH GmbH. This is an open access article under the terms of the Creative Commons Attribution Non-Commercial License, which permits use, distribution and reproduction in any medium, provided the original work is properly cited and is not used for commercial purposes.

Na_2SO_4 , this method does not apply as such, because there are two measurements but three ions. Therefore, some assumption must be done (see below), which naturally leaves some uncertainty to the fitted values.

A homogeneous membrane model is applied, although microscopic models have been presented in the literature.^[11] The bottom line of the microscopic models – originating from the Manning theory for counterion condensation in linear polyelectrolytes with charge density above a critical value – is that there exist two conducting phases, a compact phase composed of the counterions condensed on (or ion-paired to) the fixed-charge groups, and a diffuse electrical double layer around the charged linear polyelectrolytes. Ions in these two phases would assume different mobilities. As appropriate and robust these models might be, they all suffer from the need of introducing auxiliary variables, the values of which remain merely unknown fitting parameters. Alternatively, an abundance of sorption experiments, for example, with several electrolytes at varying concentrations should be done; this should be repeated when changing the membrane type. Resorting to the homogeneous membrane model means that only one parameter, the fixed membrane charge that is usually given by the manufacturer, is needed. This clearly underlines our engineering approach, i.e., the values given are averaged over several factors but represent – we believe – a reasonable estimate for process design purposes. Furthermore, we wish to show that with modern computational tools it is possible to have an easy access to the phenomena within a membrane that are otherwise hard to reach.

Theory

There are a few ways to describe solute transfer in a solution, such as the theory of irreversible thermodynamics and phenomenological equations, the Fickian approach where diffusion of neutral components is coupled with migration of charged species along their transport numbers, or the friction coefficient (Stefan-Maxwell) approach.^[10] Due to the lack of the values of the transport parameters needed in these theories, the most common and practical approach is the Nernst-Planck equation that implements the coupling of the ionic fluxes via the local electroneutrality condition and the definition of electric current.

The flux density of ionic species i is given by the Nernst-Planck equation, Eq. (1):

$$j_i = -\frac{t_i \kappa}{z_i^2 F^2} \left(RT \frac{d \ln c_i}{dx} + z_i F \frac{d\phi}{dx} \right) = -D_i \left(\frac{dc_i}{dx} + z_i c_i f \frac{d\phi}{dx} \right) \quad (1)$$

where D_i is its diffusion coefficient, z_i is its charge number, c_i is its molar concentration,

$$t_i = \frac{z_i^2 D_i c_i}{\sum_j z_j^2 D_j c_j} \quad (2)$$

is its local transport number (Eq. (2)), and

$$\kappa = \frac{F^2}{RT} \sum_j z_j^2 D_j c_j \quad (3)$$

is the electrical conductivity (Eq. (3)); $f = F/RT$.

Ions with an opposite charge to the IEM fixed charges are called counterions (subscript '1'), and are the main charge carriers via migration, while ions with the same charge, co-ions (subscript '2') are transferred mainly by diffusion in the interstitial space between the fixed charges. The concentration of a binary electrolyte (subscript '12') inside the IEM (superscript M) is defined with the co-ion, Eq. (4):

where ν_2 is the stoichiometric coefficient of the co-ion in the electrolyte. The flux density of a binary electrolyte across an IEM is given by Eq. (5):

$$J_{12}^M = -D_{12}^M \frac{dc_{12}^M}{dx} \quad (5)$$

where

$$D_{12}^M = \frac{D_1^M D_2^M (z_1^2 c_1^M + z_2^2 c_2^M)}{z_1^2 D_1^M c_1^M + z_2^2 D_2^M c_2^M} \quad (6)$$

is its diffusion coefficient (Eq. (6)). In general, the electrolyte diffusion coefficient D_{12}^M is not really a meaningful quantity as it depends on the local concentrations. In neutral or very weakly charged membranes, D_{12}^M is approximately equal to the Nernst-Hartley diffusion coefficient $\nu_{12} D_1^M D_2^M / (\nu_2 D_1^M + \nu_1 D_2^M)$, where $\nu_{12} = \nu_1 + \nu_2$. In strongly-charged IEM, $c_2^M \ll c_1^M$ and Eq. (6) reduces to $D_{12}^M \approx D_2^M$.

Eq. (5) can be integrated analytically after expressing D_{12}^M as a function of c_2^M only. Using the electroneutrality condition in Eq. (7).

$$z_1 c_1^M + z_2 c_2^M + z_M c_M = 0 \iff \frac{z_1}{z_2} c_1^M + c_2^M + X = 0 \quad (7)$$

to eliminate c_1^M , where $X = z_M c_M / z_2 > 0$, Eq. (8) is reached:

$$D_{12}^M = \frac{T_1^M c_2^M \left(1 - \frac{z_1}{z_2} \right) + T_1^M X}{c_2^M + T_1^M X} \quad ; \quad T_1^M = \frac{z_1 D_1^M}{z_1 D_1^M - z_2 D_2^M} \quad (8)$$

Integrating Eq. (5) with respect to c_2^M , the electrolyte flux density is given by Eq. (9):

$$-J_{12}^M = \frac{T_1^M}{\nu_2 h} \left\{ \left(1 - \frac{z_1}{z_2} \right) [c_2^M(h) - c_2^M(0)] + \left[1 - \left(1 - \frac{z_1}{z_2} \right) T_1^M \right] X \ln \left[\frac{c_2^M(h) + T_1^M X}{c_2^M(0) + T_1^M X} \right] \right\} \quad (9)$$

where h is the membrane thickness. The concentration drop $c_2^M(0) - c_2^M(h)$ inside the IEM is much smaller than the difference between the feed and receiver concentrations.

The conductivity of an IEM equilibrated with a binary electrolyte is given by Eq. (10):

$$\kappa^M = \frac{F^2}{RT} (z_1^2 D_1^M c_1^M + z_2^2 D_2^M c_2^M). \quad (10)$$

Hence, from Eqs. (9) and (10) and experimental measurements of J_{12}^M and κ^M , it is possible to calculate the diffusion coefficients D_1^M and D_2^M , but it requires knowing the ionic concentrations inside the IEM.

It is commonly assumed that an equilibrium of distributing ions prevails at the solution-membrane interface, i.e., $\tilde{\mu}_i^w = \tilde{\mu}_i^M$, even in the presence of electric current. Applying Guggenheim's definition of the electrochemical potential, defined by Eq. (11):

$$\tilde{\mu}_i = \mu_i^0 + RT \ln a_i + z_i F \phi, \quad (11)$$

the ionic concentration inside the IEM is now given by Eq. (12):

$$c_i^M = c_i^w \frac{\gamma_i^w}{\gamma_i^M} \exp \left[\frac{\mu_i^{0,w} - \mu_i^{0,M}}{RT} \right] \exp \left[-\frac{z_i F \Delta \phi_D}{RT} \right] \quad (12)$$

where γ_i 's refer to the activity coefficient and μ_i^0 the standard chemical potential of species i ; $\Delta \phi_D = \phi^M - \phi^w$ is the Donnan potential. Similarly, since the chemical potential of a 1:1 electrolyte is $\mu_{12} = \tilde{\mu}_1 + \tilde{\mu}_2$, its equilibrium condition at the interface is,^[37] given by Eq. (13):

$$c_1^M c_2^M = (c_{12}^w)^2 \frac{(\gamma_{\pm}^w)^2}{\gamma_1^M \gamma_2^M} \exp \left[\frac{\mu_{12}^{0,w} - \mu_{12}^{0,M}}{RT} \right] = (c_{12}^w)^2 \Gamma \quad (13)$$

where the last equality implicitly defines the factor Γ . Thus, Γ includes all the deviations from an ideal behavior, but it is rather hard to split it into activity coefficient and standard chemical potential contributions; the mean activity coefficients of aqueous electrolytes are naturally determined and tabulated in a wide concentration range. Sorption experiments can be performed to determine membrane concentrations and, therefore, Γ . From Eqs. (7) and (13), the co-ion concentration is (Eq. 14):

$$c_2^M = -\frac{X}{2} + \sqrt{\left(\frac{X}{2}\right)^2 + \Gamma (c_{12}^w)^2}. \quad (14)$$

For 2:1 and 1:2 electrolytes, c_2^M is found as the solution of a 3rd order equation that is best solved numerically. In this work, $\Gamma \equiv 1$ for the reasons discussed below.

Sulfuric acid and sodium sulfate are electrolytes with three ionic species: X^+ , XSO_4^- , and SO_4^{2-} labelled as 1 cation, 2 "bisulfate", and 3 sulfate; here, X stands for H or Na, and "bisulfate" denotes HSO_4^- or $NaSO_4^-$. The equilibrium condition of the association reaction is $\mu_2 = \mu_1 + \mu_3$, which is equivalent to Eq. (15)

$$K_c = \frac{c_1 c_3}{c_2}. \quad (15)$$

The chemical potential of the electrolyte is given by Eq. (16):

$$\mu_5 = \mu_1 + \mu_2 = 2\mu_1 + \mu_3. \quad (16)$$

In this work, the theoretical analysis of the diffusion experiments of H_2SO_4 and Na_2SO_4 has been done using two procedures. The first one consists of the numerical solution of the ionic transport equations, Eq. (1), using COMSOL Multiphysics simulations as described in detail in Ref [35]. The second procedure consists of deducing the Fick equation, Eq. (17):

$$J_s = -D_5 \frac{dc_5}{dx} \quad (17)$$

for these electrolytes, and then numerically integrating Eq. (17). In both cases, we have to take into account that the equilibrium "constant" K_c is a function of the electrolyte concentration,^[37] because Eq. (15) is written in terms of the molar concentrations, c_i , rather than the ionic activities. We explain next the second procedure.

In diffusion experiments the electric current density is zero, $0 = \sum_i z_i j_i$, and the (diffusion) electric potential gradient of these ternary electrolytes is given by Eq. (18):

$$-F \frac{d\phi}{dx} = t_1 \frac{d\mu_1}{dx} - t_2 \frac{d\mu_2}{dx} + \frac{t_3}{2} \frac{d\mu_3}{dx} = -\frac{d\mu_2}{dx} + \left(t_1 + \frac{t_3}{2} \right) \frac{d\mu_5}{dx} - \frac{1}{2} \frac{d\mu_3}{dx} + \frac{t_1 - t_2}{2} \frac{d\mu_5}{dx} \quad (18)$$

where we have used Eq. (12). Introducing $d\phi/dx$ from Eq. (18) into Eq. (1) for the "bisulfate" and sulfate ions, their flux densities are Eqs. (19) and (20):

$$j_2 = -\frac{t_2 \kappa}{F^2} \left(\frac{d\mu_2}{dx} - F \frac{d\phi}{dx} \right) = -\frac{t_2 \kappa}{F^2} \left(t_1 + \frac{t_3}{2} \right) \frac{d\mu_5}{dx} \quad (19)$$

$$j_3 = -\frac{t_3 \kappa}{4F^2} \left(\frac{d\mu_3}{dx} - 2F \frac{d\phi}{dx} \right) = -\frac{t_3 \kappa}{4F^2} (t_1 - t_2) \frac{d\mu_5}{dx}. \quad (20)$$

Under steady-state conditions, the flux densities j_2 and j_3 vary with position due to the association reaction of cation and sulfate to form "bisulfate". On the contrary, the sulfate constituent flux density is Eq. (21):

$$J_s = j_2 + j_3 = -\frac{\kappa}{F^2} \left[t_1 t_2 + \frac{1}{4} (t_1 + t_2) t_3 \right] \frac{d\mu_5}{dx} - \frac{D_2 D_3 c_2 c_3 + D_1 D_3 c_1 c_3 + D_1 D_2 c_1 c_2}{D_1 c_1 + D_2 c_2 + 4D_3 c_3} \frac{1}{RT} \frac{d\mu_5}{dx} \quad (21)$$

does not vary with position. Eq. (21) can be transformed to Eq. (17).

The ionic concentrations vary with position inside the IEM, but the concentration gradients are relatively small in strongly

charged membranes. Therefore, in order to obtain an analytical expression of the diffusion coefficient D_5 of the electrolyte, it is reasonable to assume that K_c is constant. By differentiating Eq. (15) and the local electroneutrality condition, we have Eqs. (22) and (23):

$$\frac{1}{c_2} \frac{dc_2}{dx} = \frac{1}{c_1} \frac{dc_1}{dx} + \frac{1}{c_3} \frac{dc_3}{dx} \quad (22)$$

$$\frac{dc_1}{dx} = \frac{dc_2}{dx} + 2 \frac{dc_3}{dx} \quad (23)$$

Combining Eqs. (22) and (23), the gradient of the chemical potential of the electrolyte, Eq. (16), is given by Eq. (24):

$$\frac{1}{RT} \frac{d\mu_5}{dx} = \frac{1}{RT} \frac{d\mu_5}{dc_5} \frac{dc_5}{dx} = \frac{c_1 + c_2 + 4c_3}{c_2c_3 + c_1c_3 + c_1c_2} \frac{dc_5}{dx} \quad (24)$$

where $c_5 = c_2 + c_3$ is the stoichiometric electrolyte concentration. Thus, from Eqs. (21) and (24), the electrolyte diffusion coefficient can be identified as Eq. (25):

$$D_5 = \frac{D_2D_3c_2c_3 + D_1D_3c_1c_3 + D_1D_2c_1c_2}{D_1c_1 + D_2c_2 + 4D_3c_3} \frac{c_1 + c_2 + 4c_3}{c_2c_3 + c_1c_3 + c_1c_2} = \frac{\frac{D_2D_3}{c_1} + \frac{D_1D_3}{c_2} + \frac{D_1D_2}{c_3}}{\frac{1}{c_1} + \frac{1}{c_2} + \frac{1}{c_3}} \frac{c_1 + c_2 + 4c_3}{D_1c_1 + D_2c_2 + 4D_3c_3} \quad (25)$$

Although there is no simple, concentration-independent expression for D_5 , Eq. (17) can be formally integrated between the membrane boundaries as Eq. (26):

$$J_5 h = \int_{c_5(h)}^{c_5(0)} D_5 dc_5^w \quad (26)$$

because J_5 does not vary with position. At $x = 0$ the IEM is in equilibrium with an external feed solution with electrolyte concentration $c_5(0)$. At $x = h$ the IEM is in equilibrium with an external receiver solution with electrolyte concentration $c_5(h) \leq c_5(0)$. For any position $0 \leq x \leq h$, the local ionic concentrations inside the IEM can be considered to stay in equilibrium with a virtual external solution with electrolyte concentration c_5^w , such that $c_5(0) \leq c_5^w \leq c_5(h)$. For every value of c_5^w , the ionic concentrations inside an IEM with a concentration c_M of fixed charge groups of charge number z_M can be evaluated as follows. First, we calculate the three local ionic concentrations c_1^w , c_2^w and c_3^w in the virtual external solution (corresponding to position x) as the solution of three equations: the definition $c_5^w = c_2^w + c_3^w$ of the electrolyte concentration, electroneutrality $c_1^w = c_2^w + 2c_3^w$, and association equilibrium $K_c(c_5^w) = c_1^w c_3^w / c_2^w$. The local ionic concentrations inside the IEM are $c_1^M = c_1^w e^{-\varphi}$, $c_2^M = c_2^w e^{\varphi}$ and $c_3^M = c_3^w e^{2\varphi}$, where $\varphi = f\Delta\phi_D$ can be determined from the condition of local electroneutrality inside the IEM, $z_M c_M + c_1^M = c_2^M + 2c_3^M$. Thus, for every c_5^w , we can evaluate c_1^M , c_2^M and c_3^M and hence D_5 from Eq. (26). From the numerical evaluation of the integral in Eq. (26), the electrolyte

flux density J_5 across an IEM separating solutions with concentrations $c_5(0)$ and $c_5(h)$ can be calculated.

The calculations of the dissociation equilibria of NaSO_4^- and HSO_4^- with sulfate are described in Supporting Information. The key finding is that the concentration-based dissociation constant, K_c , is substantially higher than the thermodynamic dissociation constant, K_a , and, hence, ignoring the activity correction in the ionic equilibria would cause significant errors.

Experimental Section

Materials

Sodium sulfate (Fluka, purity >99.0% (Germany)), sulfuric acid (Merck KGaA with MQ 100 (Germany)), NaOH (Merck KGaA pellets p.a. grade EMSURE® (Germany)), NaCl (Scharlau reagent grade ACS, ISO, Reag. Ph Eur), and HCl 32% (Merck KGaA p.a. grade EMSURE® (Germany)) are used as received.

AR103P and CR61P from Suez Water Technologies and Solutions are reinforced membranes composed of inert reinforcing fibers and ion-exchange resins.^[1] The chemical structures of their ion-exchange polyelectrolytes are shown, in Ref. [38], Ref. [39]. The properties listed in Table 1 include data from the manufacturer and calculated values. The water content WC of the hydrated ion-exchange resin is the mass fraction of the water in the hydrated ion-exchange resin (not counting the inert reinforcing fibers), $WC = m_w/m_m$ (from the manufacturer). The water uptake of the dry ion-exchange resin is the ratio of the mass of sorbed water to the mass of the dry ion-exchange resin, $WU = m_w/m_{dm} = WC/(1 - WC)$. The volume fraction of water in the hydrated ion-exchange resin is $\phi_w = V_w/V_m = WC\rho_m/\rho_w$, where ρ_m is the density of the hydrated ion-exchange resin and ρ_w is the density of water. The ion-exchange capacity $c_{\text{ie}}^{\text{ex}}$ is the ratio of the number of fixed-charge groups and the mass m_{dm} of the dry ion-exchange resin.

We use a homogeneous membrane model, that is, the membrane is considered as a homogeneous phase composed of ion-exchange resin, water and ions, with no pores or structural features. The hydrophobic reinforcing fibers are not considered as part of the membrane as they are irrelevant for ionic transport. The membrane fixed charge concentration [Eq. (27)]

$$c_M = \frac{c_{\text{ie}}^{\text{ex}} m_{\text{dm}}}{V_w} = \frac{c_{\text{ie}}^{\text{ex}} \rho_m}{(1 + WU)\phi_w} = \frac{c_{\text{ie}}^{\text{ex}} \rho_m (1 - WC)}{\phi_w} \quad (27)$$

is the number of fixed-charge groups per volume of sorbed water. The values of c_M shown in Table 1 have been calculated using $\rho_m \approx 1.0 \text{ g/mL}$ and $\phi_w \approx 0.4$. Alternatively, $\phi_w = WU/(WU + \rho_w/\rho_{\text{dm}})$ and $1/\rho_m = (1 - WC)/\rho_{\text{dm}} + WC/\rho_w$ could be used, with the density ρ_{dm} of the dry ion-exchange resin reported in Ref. [39].

Table 1. Characteristics of the membranes.^[1]

membrane (type)	area [cm ²]	thickness [μm]	WC	WU	$c_{\text{ie}}^{\text{ex}}$ [meq/g]	c_M [M]
AR103P (AEM)	10	570	0.39	0.639	2.37	3.6
CR61P (CEM)	10	580	0.44	0.786	2.20	3.1

Diffusion Experiments

Diffusion experiments were carried out in a two-compartment cell setup with a single IEM separating them. The electro dialysis cell (Micro Flow Cell, Electrocell, Denmark) is assembled with IEMs, two leak-free reference electrodes (LF-1, 1 mm OD, Ag/AgCl from Alvatek, United Kingdom), as well as Pt coated Ti anode and cathode (Figure 1). The active membrane and electrode area are 10 cm² and the membrane spacing is 3 mm. The flow rate was 100 mL/min for each liquid channel (width 3 mm) and was controlled by peristaltic pumps (Watson Marlow 323). The feed compartment concentration was 0.25 M and the receive compartment concentration was 0.01 M. The membrane was immersed in 0.25 M electrolyte first for 24 h. Electrolyte diffusion was monitored by measuring the conductivity of both compartments with WTW TetraCon 925 conductometer. Conductivities were then converted to concentrations with the data from the CRC Handbook of Chemistry and Physics.^[40] The concentration of feed and products were also verified by titration with Titrette® 25 mL class A precision.

Resistance Measurements

A variable number N (from 1 to 4) of membranes (IEM*) was placed between two auxiliary IEMs (Figure 2). The distance between two reference electrodes was 1.7 mm with one membrane and changed accordingly by the number of membranes. All membranes were equilibrated with the electrolytes (0.15 M) for 24 h prior to the measurements. Spacers were placed in the compartments to cause turbulence close to the membrane surface. The total electrical resistance [Eq. (28)]

$$R_{\text{TOT}} = NR^{\text{M}} + R_{\text{aux}} \quad (28)$$

of the cell was measured in 0.15 M HCl, NaOH, NaCl, H₂SO₄, and Na₂SO₄ using EIS, as the intercept on the real axis of the Nyquist plot. The auxiliary resistance R_{aux} consists of the electrode and solution resistances. The resistance R^{M} of a single membrane (IEM*) was obtained by fitting the R_{TOT} vs. N measurements to Eq. (28). Due to the imperfectly smooth surface of the membranes, R^{M} may contain a small contribution associated to the solution layer between membranes. The impedance measurements were carried out with an AUTOLAB PGSTAT128 N potentiostat and Nova 2.1 software. The impedance spectra were measured at the open circuit potential with an AC amplitude of 10 mV and a frequency range from 10 kHz to 0.5 Hz.

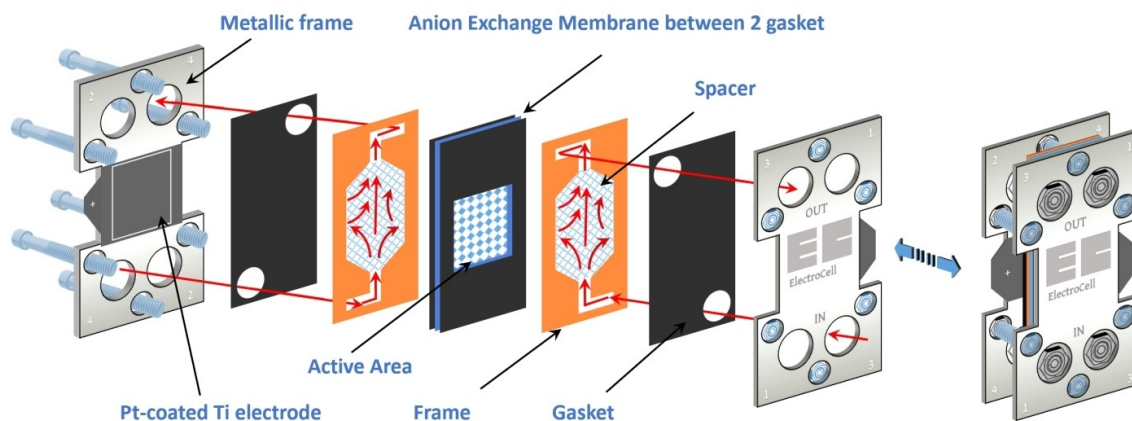


Figure 1. ElectroCell used for diffusion experiments.

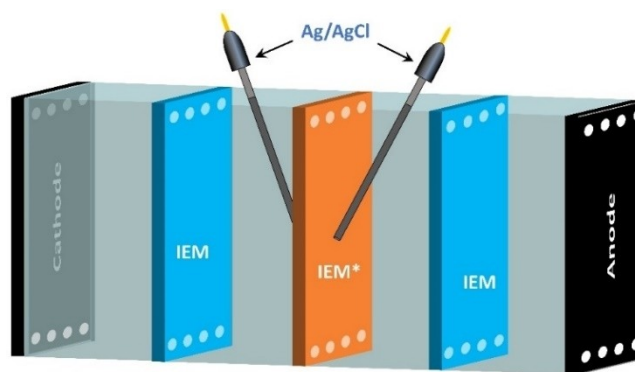


Figure 2. Schematic representation of membrane resistance measurement.

Scanning Electron Microscopy (SEM)

The membranes were imaged using a scanning electron microscope Tescan Mira3. A high voltage of 2–5 kV was applied to the specimen. In this study, a low-vacuum mode was used with the backscattering of electrons. The sputtering of membrane surface was also carried out using Quorum Q150T ES before SEM. The purpose of sputtering was to increase the surface conductivity of the membranes. In general, the non-conductive surface acts as an electron trap, which results in the accumulation of electrons on the surface is called “charging”.^[41] The conductive coated material acts as a path that allows the charging electrons to be removed from the membrane surface. The charging electrons cause extra-white regions on the sample, which can influence the image information and quality. Au–Pd was used as a conductive material layer. Pure argon was used as a backfill process gas.

The AR103P and CR61P membranes are identical in most aspects, such as thickness, color, and chemical stability. The orthogonal cross-section images (Figures 3a and 3c) depict the ion-exchange resin between the supporting polymer reinforcing fiber web (diameter 20 μm). This morphology becomes highly conductive when immersed in an electrolyte. Furthermore, free leakage of electrolytes is not possible due to their tightly packed structure. The visible surface cracks are due to drying of both membranes (Figures 3b and 3d) before SEM imaging.

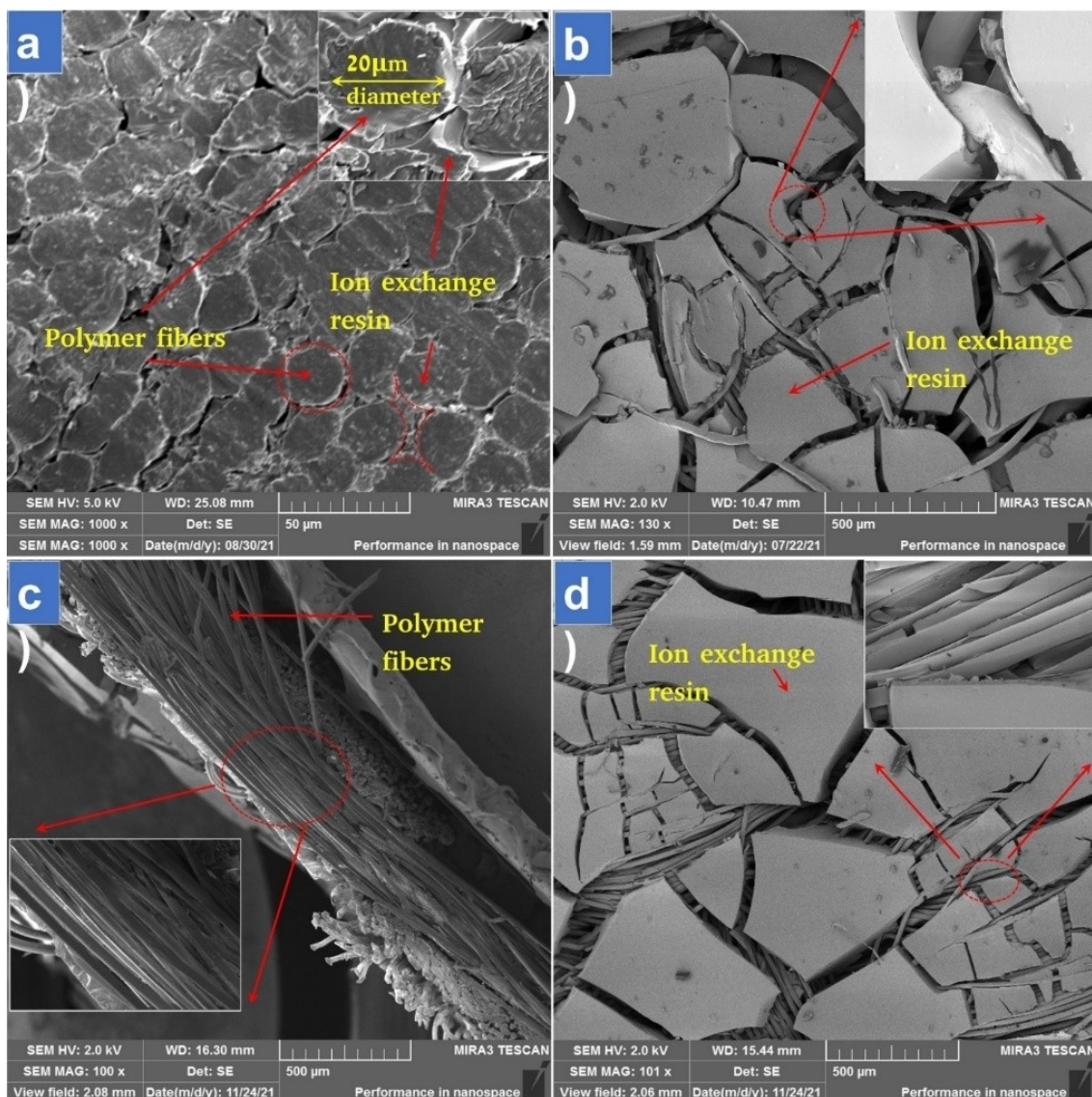


Figure 3. Cross-section (a) and surface (b) SEM images of AR103P. Cross-section (c) and surface (d) SEM images of CR61P.

Result and Discussion

Figure 4 shows the concentration changes in the receiver compartments during diffusion experiments. As anticipated, acids (HCl, H_2SO_4) diffuse in an AEM significantly faster than salts (NaCl , Na_2SO_4), because of the high mobility of proton. Furthermore, sulfuric acid shows an exponential concentration rise, while the concentrations of the other electrolytes are changing more gradually, almost in a linear fashion. The observed diffusion rate in AEM is $\text{H}_2\text{SO}_4 > \text{HCl} > \text{NaCl} > \text{Na}_2\text{SO}_4 > \text{NaOH}$, whereas for CEM it is $\text{NaOH} > \text{HCl} > \text{NaCl} > \text{Na}_2\text{SO}_4 \geq \text{H}_2\text{SO}_4$. From this trend, the membrane conductivity behavior is also predicted.

An interesting and perhaps a bit surprising observation is that, in the CEM, the flux of NaOH is twice as high as that of NaCl and much higher than that of H_2SO_4 , underlining the fact that the co-ion defines mainly the rate of diffusion. The mobility

of sulfate (or bisulfate) in a CEM is lower than that of OH^- or Cl^- . Similar results were reached by Kiyono et al.^[42] and Wycisk et al.^[43] Comparison of NaCl and HCl fluxes also makes sense because of the higher mobility of protons.

In the AEM, on the contrary, NaOH appears to diffuse the most slowly, even more slowly than Na_2SO_4 . From the Donnan equilibrium calculations, the concentration difference across the AEM was found to be for Na_2SO_4 ca. 5-fold to that of NaOH. The ultimate reason for this is the Donnan equilibrium that was on the feed side was ca. 25 mV for Na_2SO_4 and ca. 70 mV for NaOH, because the Donnan potential is lower when the counterion is divalent. The higher the Donnan potential is, the more it equalizes concentration differences across the membrane. Hence, when analyzing flux data, looking at the diffusion rates only does not suffice, but the chemistry behind them must be understood as well.

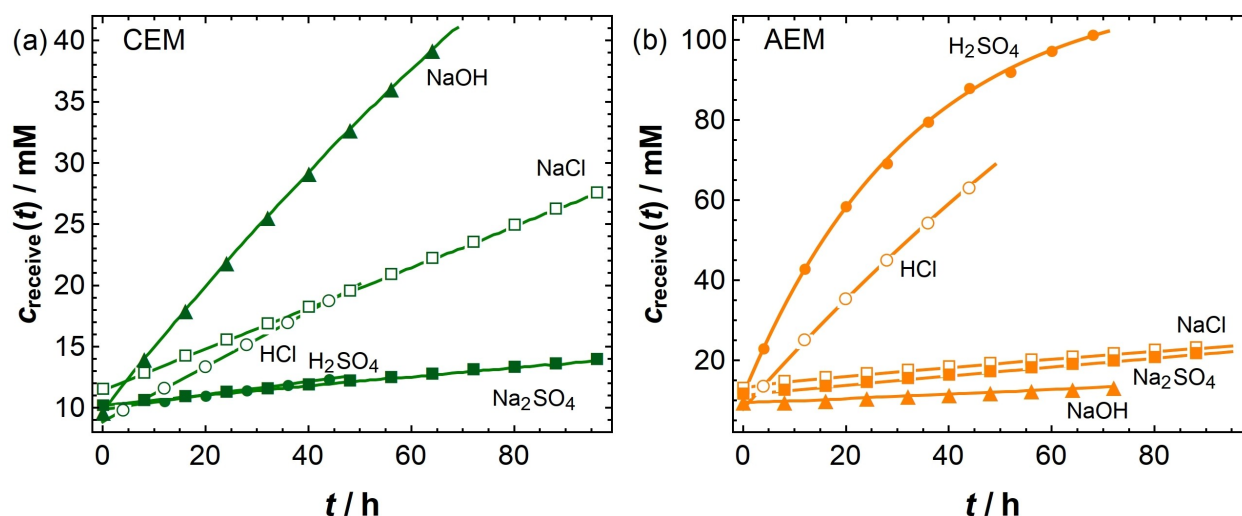


Figure 4. Receive compartment concentration in diffusion experiments a) CEM, b) AEM. [system = Feed (0.25 M) | Membrane | Receive (0.01 M)]

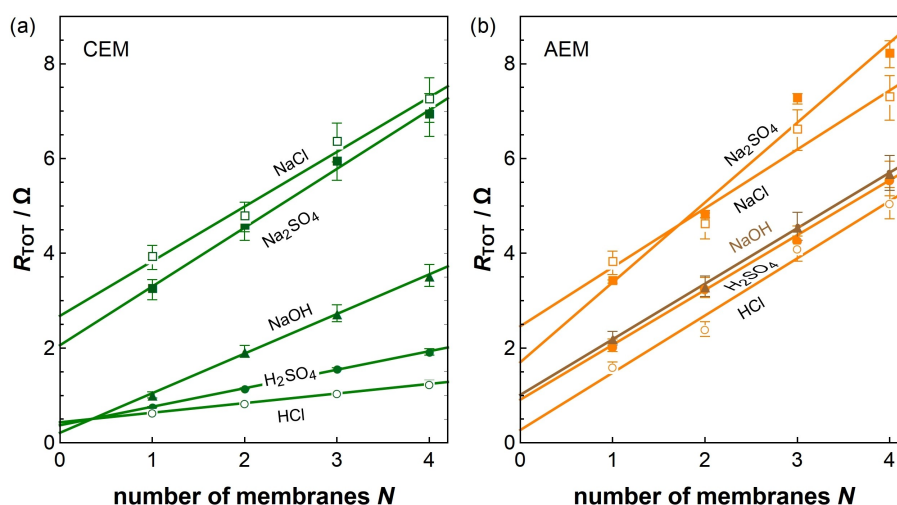


Figure 5. Resistances of cells with stacked IEMs and various electrolytes.

The electrolyte flux density is determined from the mass balance as Equation (29):

$$J_{12} = \frac{V}{A} \left(\frac{dc}{dt} \right)_{t=0} \quad (29)$$

where V is the volume of the feed or the receiver compartment and A is the geometrical area of the membrane. The term $(dc/dt)_{t=0}$ is the initial slope of the concentration vs. time curve. The initial slope was determined by fitting the receiver compartment concentration to an exponential function of time and calculating its derivative at $t=0$. This is done because the concentration in the receiver (feed) compartment increases (decreases) in an exponential manner. Also, when comparing measurements with COMSOL simulations where concentrations were fixed at the limits of the simulation domain, the initial flux is needed.

The resistance between the reference electrodes in different electrolytes is plotted against the number of membranes (IEM*) in Figure 5. The dependence is linear, as expected. The auxiliary resistance is obtained from the intercept of the plots. Because of the relatively higher mobility of proton and hydroxide, the membrane conductivity is noticeably higher when the electrolyte is an acid or base (NaOH, HCl, H₂SO₄) than when it is salt (NaCl, Na₂SO₄, Figure 6).

From the results of the diffusion experiments and the electrical resistance R^M measurements, J_{12}^M and $\kappa^M = h/AR^M$ are determined. Inserting these values in Eqs. (9) and (10), we have a system of two equations that can be numerically solved to obtain the two unknowns¹, D_+^M and D_-^M , e.g., using Mathematica®. The diffusion coefficient of co-ions is higher than that of counterions with the exception of H⁺ in the CEM, which is not

¹ Here we use, for the case of clarity, symbols D_+ and D_- because cations are counter-ions in the CEM but co-ions in the AEM, and anions vice versa.

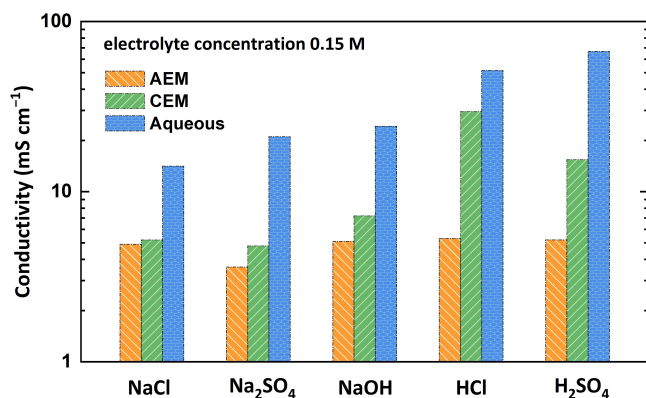


Figure 6. Conductivities of the IEMs in the studied electrolytes (0.15 M).

surprising because of its high mobility. Also, it is commonly observed that proton leakage through AEMs is quite high, as we observed in our previous paper.^[35] Also, the higher mobility of OH⁻ seems to agree with its leakage through the CEM.^[35]

In the CEM, the diffusion coefficients of the counterion are ca. 3–4% of their aqueous values at infinite dilution, while in the AEM it is only of the order of 1–2% because of the higher fixed charge density (Figure 7). The diffusion coefficients of the co-ions are 7–9% and 4–16% of their aqueous values at infinite dilution in the CEM and AEM, respectively (Table 2). It has to be emphasized that the values are averaged over the sorbed water volume and, thus, do not provide values for the condensed phase and free counter-ions separately.

The procedure for the determination of the diffusion coefficients of the ionic species in Na₂SO₄ and H₂SO₄ is explained in the Theoretical section. Because there are two experimental quantities, the diffusion flux and the conductivity,

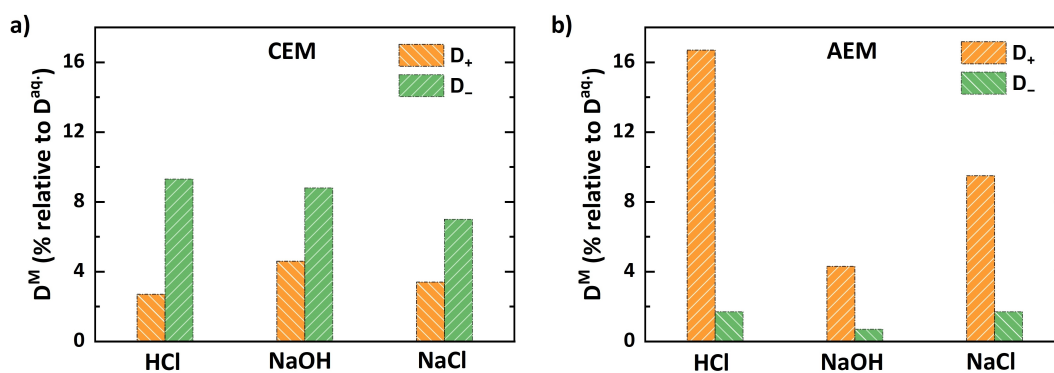


Figure 7. Comparison of ionic diffusion coefficients in a) CEM, b) AEM in different strong electrolytes.

electrolyte	CEM, $c_M = 3.1$ M		AEM, $c_M = 3.6$ M	
	D_+^M	D_-^M	D_+^M	D_-^M
NaCl	0.44 (3.4)	1.40 (7.0)	1.23 (9.5)	0.35 (1.7)
NaOH	0.60 (4.6)	4.57 (8.8)	0.56 (4.3)	0.37 (0.7)
HCl	2.51 (2.7)	1.86 (9.3)	15.6 (16.7)	0.34 (1.7)

Table 3. The ionic diffusion coefficients [10^{-7} cm² s⁻¹] of weak electrolytes: subscript 1 refers to H⁺ or Na⁺, 2 to HSO₄⁻ or NaSO₄⁻, and 3 to SO₄²⁻. Notation similar to Table 2.

electrolyte	CEM, $c_M = 3.1$ M			AEM, $c_M = 3.6$ M		
	D_1^M	^[a] D_2^M	D_3^M	D_1^M	^[b] D_2^M	D_3^M
Na ₂ SO ₄	4.11 (3.1)	5.60 (4.3)	4.30 (4.3)	1.21 (0.9)	1.21 (0.9)	1.32 (1.3)
H ₂ SO ₄	13.2 (1.4)	5.42 (4.17)	4.17 (4.17)	56.8 (6.1)	7.94 (6.1)	1.19 (1.9)

[a] $D_2^M/D_2^w = D_3^M/D_3^{w*}$, [b] $D_1^M/D_1^w = D_2^M/D_2^w$.

but three diffusion coefficients, an extra assumption, as indicated in the Table 3, is needed to solve the problem.

Solving the ternary case equation (26) numerically is quite tedious and demanding. Using COMSOL Multiphysics it can be avoided because a user does not need to solve any equations or write a computing script, but choosing an appropriate model from a menu, in this case the Nernst-Planck equation with electroneutrality, suffices. Naturally, fundamental understanding of physics and chemistry is required to set-up a meaningful model. We described these calculations in detail in our previous paper.^[35] Briefly: Ternary Current Distribution module was applied with the Donnan boundary conditions at the solution-membrane interfaces; the sulfate dissociation equilibria were incorporated as a reaction term in the steady-state transport equations; at the limits of the simulation domain the concentrations of the species were fixed; at one limit the Galvani potential was set to zero and at another limit electric current was set to zero, hence ensuring pure diffusion.

Simulations of the conductivity measurement, keeping the solution concentrations equal on both sides of the membrane, showed that in the case of H₂SO₄ and the CEM, the only meaningful species in the membrane is H⁺. Therefore, from the

measured conductivity the diffusion coefficient of H^+ was readily found (Table 3). This value was then used to simulate the diffusion experiment, keeping the ratio D_2/D_3 the same in the solution and membrane phases. In the case of Na_2SO_4 and the CEM, the conductivity is determined by Na^+ because the concentrations of the sulfate species are very low, ca. 2.0 mM only. Hence, D_1^M was readily found and keeping again the ratio D_2/D_3 constant they were found from the diffusion flux.

In the case of Na_2SO_4 and AEM, sulfate determines the conductivity almost entirely (98%) which leads to the value of D_3^M , and applying the constraint as indicated the other diffusion coefficients were found. The most tedious case was H_2SO_4 with the AEM, because all the ions have non-negligible contributions to the conductivity. The ionic diffusion coefficient values that showed agreement between the measured electrolyte diffusion flux density and that calculated with Eq. (26), using a Mathematica script, were inserted in the COMSOL model, and an agreement within the accuracy of the measurements (ca. 5%) were reached. The high mobility of proton, causing leakage across AEMs is again seen in its diffusion coefficient that stands out from Table 3.

It has to be realized that the values given in Table 3 are very good estimates, not absolute ones. Previously,^[35] we assumed that the diffusion coefficient values were 10% of their aqueous values at infinite dilution, except for proton 60%. In that work the diffusion coefficients were corrected for the free volume (40%) and the tortuosity (1.5) of the membrane which makes a coefficient 3.75, i.e. 10% becomes ca. 2.7% and 16% for proton. Hence, we can conclude that the assumption was quite appropriate considering that with electric current the main transport mechanism is migration. Looking at Eq. (2) it is obvious that when all diffusion coefficients are scaled with the same number, the transport number does not change at all.

One of the advantages of COMSOL simulations is that it is possible to look at the components of the flux density separately, which would be very hard in an analytical solution or when writing a computing script. For any electrolyte with different diffusion coefficients of counterions and co-ions, in the

absence of electric current a diffusion potential is developed across the IEM. Thus, the electrolyte flux density, when written in terms of ionic flux densities, consists of diffusional and migration contributions. For the case of sulfuric acid, the contributions [Eqs. (30) and (31)]

$$J_{s,dif} = j_{2,dif} + j_{3,dif} = -D_2 \frac{dc_2}{dx} - D_3 \frac{dc_3}{dx} \quad (30)$$

$$J_{s,mig} = j_{2,mig} + j_{3,mig} = (D_2 c_2 + 2D_3 c_3) F \frac{d\phi}{dx} \quad (31)$$

are shown in Figure 8. The migration contribution is actually higher than the diffusional one.

Finally, it must be realized that a concentration difference across an IEM creates an osmotic pressure difference that causes water flow in the opposite direction of the diffusion flux. In our previous paper,^[35] we measured the volume change due to electroosmosis at varying current densities. The volume changes were 1–20 mL in 2 h. If we extrapolate this data to zero current density, a definite value cannot be given but it appears to be very small. Therefore, osmosis was ignored in the current study.

In Eq. (13) the parameter Γ , including all the deviations from ideal behavior, was introduced. As can be seen, it contains both the activity coefficient corrections and the standard chemical potential difference. Kamcev et al.^[36] assumed that the standard chemical potentials were equal in the aqueous and membrane phases and that Eq. (32)

$$\Gamma = \frac{(\gamma_{\pm}^M)^2}{\gamma_1^M \gamma_2^M} \quad (32)$$

can be calculated from electrostatics using Manning's condensation theory. Calculating the denominator in Eq. (32) requires the parameter $\xi = \lambda_B/b$, the ratio of the Bjerrum length, λ_B , and the average distance between the fixed charge groups, b . The parameter b would probably vary around 10 Å, and the Bjerrum

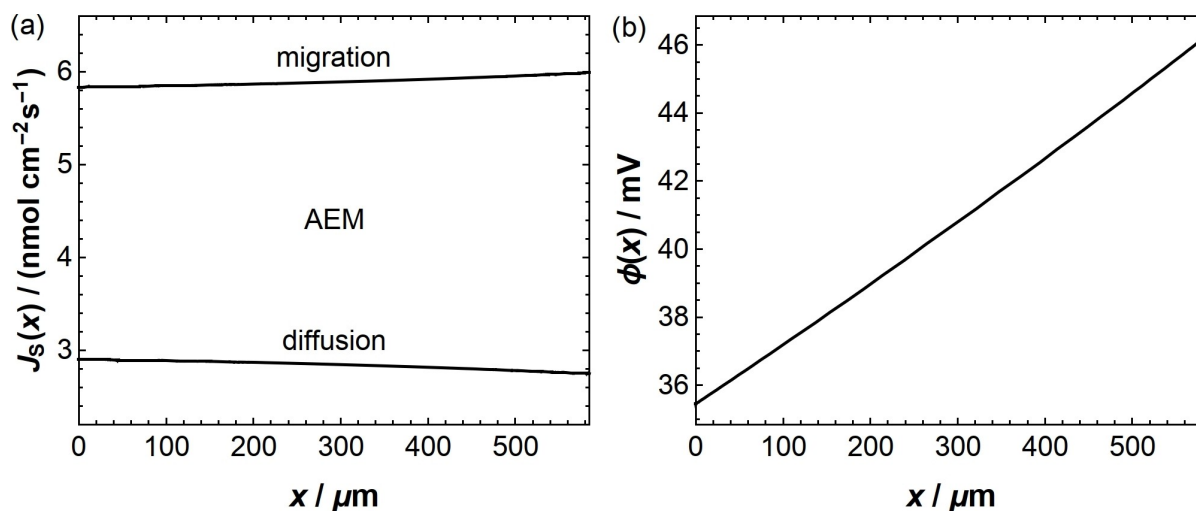


Figure 8. a) Diffusion and migration contributions of the sulfate constituent flux in the AEM. b) Potential profile across the AEM.

length depends on the relative permittivity inside the membrane pores. Hence, Γ would vary significantly on the choice of these parameters. The theory applies to strong binary electrolytes, not to our cases with Na_2SO_4 and H_2SO_4 . Also, the deviations from ideal behavior are not only electrostatic in nature and they should include specific interactions between an ion and a membrane. In aqueous solutions the standard chemical potential μ^0 reflects the hydration energy of an ion, which also depends on the relative permittivity of the medium. Therefore, due to the uncertainty of its accurate value, we are not accounting for the effect of Γ . Its effect on the concentration gradient in the membrane or its conductivity would not be any larger than the inherent uncertainty of the experimental data.

Conclusions

The diffusion of various ions across the IEMs is studied and diffusion coefficient values of different electrolytes are experimentally determined. The main aim of the study was to understand the mobility of different ions through fixed-charged IEMs at zero current. The diffusion fluxes of various electrolytes across an anion and a cation exchange membrane were measured and combining that data to the membrane resistance at a constant concentration, the individual ionic diffusion coefficients were determined. Donnan equilibria at the solution-membrane interfaces were assumed, ignoring the possible differences of the standard chemical potentials and activity coefficients between the aqueous and membrane phases. In our case, highly charged membranes were used, and the electrolyte diffusion coefficient inside the IEM is found very close to the co-ion diffusion coefficient. Ionic diffusion coefficients in the membrane were found not a single-valued quantity but depends slightly on the environment; their values are roughly 2–7% of their aqueous values at infinite dilution.

The analysis of sulfuric acid diffusion and conductance data is hampered by the dissociation equilibrium of bisulfate which prevents the use of the Nernst-Hartley equation. Therefore, the estimation of the bisulfate mobility was done by iterating its value to match the experimental acid flux that was calculated in terms of the sulfate constituent.

It has to be emphasized that the values here obtained are apparent ones, i.e., they include the contributions of the porosity and tortuosity of the membrane that cannot be easily distinguished from each other. Hence, if these parameters vary significantly from those of the membranes here used, corresponding modifications need to be done. In the analysis of the data, the Donnan equilibrium plays a salient role, as the concentration gradient in the membrane is affected by the membrane charge and thus by the Donnan potential.

Acknowledgements

This work has received funding from the European Union, EIT Raw Materials project Credit-18243. SUEZ Water Technologies and

Solutions is acknowledged for the supply of the membranes. Mr. Heikki Pajari (Sr. Scientist at VTT Technical Research Centre of Finland Ltd) is acknowledged for commenting on the manuscript. J.A.M acknowledges the funding from project PID2021-126109-NB-I00, Ministry of Science and Innovation (Spain), and FEDER.

Conflict of Interest

The authors declare no conflict of interest.

Data Availability Statement

The data that support the findings of this study are available from the corresponding author upon reasonable request.

Keywords: ionic transport · ionic diffusion · ion-exchange membranes · COMSOL Multiphysics · diffusion coefficients

- [1] Kuldeep, W. D. Badenhurst, P. Kauranen, H. Pajari, R. Ruismäki, P. Mannela, L. Murtoimäki, *Membranes* **2021**, *11*, 718.
- [2] B. E. Logan, M. Elimelech, *Nature* **2012**, *488*, 313.
- [3] S. Porada, R. Zhao, A. van der Wal, V. Presser, P. M. Biesheuvel, *Prog. Mater. Sci.* **2013**, *58*, 1388.
- [4] H. Strathmann, *Ion-exchange Membrane Separation Processes*, Elsevier, Amsterdam, **2004**.
- [5] Y. Leng, G. Chen, A. J. Mendoza, T. B. Tighe, M. A. Hickner, C.-Y. Wang, *J. Am. Chem. Soc.* **2012**, *134*, 9054.
- [6] E. A. Hernández-Pagán, N. M. Vargas-Barbosa, T. Wang, Y. Zhao, E. S. Smotkin, T. E. Mallouk, *Energy Environ. Sci.* **2012**, *5*, 7582.
- [7] A. Heinzl, V. M. Barragán, *J. Power Sources* **1999**, *84*, 70.
- [8] E. Ji, H. Moon, J. Piao, P. T. Ha, J. An, D. Kim, J.-J. Woo, Y. Lee, S.-H. Moon, B. E. Rittmann, I. S. Chang, *Biosens. Bioelectron.* **2011**, *26*, 3266.
- [9] M. Y. Kariduraganavar, R. K. Nagarale, A. A. Kittur, S. S. Kulkarni, *Desalination* **2006**, *197*, 225.
- [10] K. Kontturi, L. Murtoimäki, J. A. Manzanares, *Ionic Transport Processes in Electrochemistry and Membrane Science*, Oxford University Press, Oxford, **2015**.
- [11] R. P. Buck, *J. Membr. Sci.* **1984**, *17*, 1.
- [12] R. B. Bird, W. E. Stewart, E. N. Lightfoot, *Transport Phenomena*, John Wiley & Sons, **2006**.
- [13] M. Lopez, B. Kipling, H. L. Yeager, *Anal. Chem.* **1976**, *48*, 1120.
- [14] C. R. C. Wang, J. W. Strojek, T. Kuwana, *J. Phys. Chem.* **1987**, *91*, 3606.
- [15] Z. Samec, A. Trojánek, J. Langmaier, E. Samcová, *J. Electrochem. Soc.* **1997**, *144*, 4236.
- [16] Z. Samec, A. Trojánek, E. Samcová, *J. Electroanal. Chem.* **1995**, *389*, 1.
- [17] S. Koter, A. Narébska, *Electrochim. Acta* **1987**, *32*, 455.
- [18] P. Millet, *J. Membr. Sci.* **1990**, *50*, 325.
- [19] G. Pourcelly, A. Oikonomou, C. Gavach, H. D. Hurwitz, *J. Electroanal. Chem.* **1990**, *287*, 43.
- [20] P. C. Rieke, N. E. Vanderborgh, *J. Membr. Sci.* **1987**, *32*, 313.
- [21] D. N. Amang, S. Alexandrova, P. Schaezel, *Electrochim. Acta* **2003**, *48*, 2563.
- [22] H. L. Yeager, B. Kipling, *J. Phys. Chem.* **1979**, *83*, 1836.
- [23] M. W. Verbrugge, R. F. Hill, *J. Electrochem. Soc.* **1990**, *137*, 886.
- [24] M. W. Verbrugge, E. W. Schneider, R. S. Conell, R. F. Hill, *J. Electrochem. Soc.* **1992**, *139*, 3421.
- [25] K. Sato, T. Yonemoto, T. Tadaki, *J. Membr. Sci.* **1990**, *53*, 215.
- [26] F. G. Helfferich, *Ion Exchange*, Dover, New York, **1995**.
- [27] J. Crank, G. S. Park, *Diffusion in Polymers*, Academic Press, London, New York, **1968**.
- [28] N. Lakshminarayanaiah, *Transport Phenomena in Membranes*, New York, Academic Press, **1969**.
- [29] V. I. Volkov, A. V. Chernyak, I. A. Avilova, N. A. Slesarenko, D. L. Melnikova, V. D. Skirda, *Membranes* **2021**, *11*, 385.

- [30] C. Yin, S. Wang, Y. Zhang, Z. Chen, Z. Lin, P. Fu, L. Yao, *Environ. Sci.: Water Res. Technol.* **2017**, *3*, 1037.
- [31] F. Müller, C. A. Ferreira, D. S. Azambuja, C. Alemán, E. Armelin, *J. Phys. Chem.* **2014**, *118*, 1102.
- [32] V. V. Nikonenko, A. E. Kozmai, *Electrochim. Acta* **2011**, *56*, 1262.
- [33] Z. Zhao, S. Shi, H. Cao, Y. Li, *J. Membr. Sci.* **2017**, *530*, 220.
- [34] T. C. Chilcott, A. Antony, G. Leslie, *Desalination* **2017**, *403*, 64.
- [35] Kuldeep, P. Kauranen, H. Pajari, R. Pajarre, L. Murtomäki, *Chem. Eng. J.* **2021**, *8*, 100169.
- [36] J. Kamcev, M. Galizia, F. M. Benedetti, E.-S. Jang, D. R. Paul, B. D. Freeman, G. S. Manning, *Phys. Chem. Chem. Phys.* **2016**, *18*, 6021.
- [37] E. B. Robertson, H. B. Dunford, *J. Am. Chem. Soc.* **1964**, *86*, 5080.
- [38] J. Kamcev, D. R. Paul, G. S. Manning, B. D. Freeman, *Macromolecules* **2018**, *51*, 5519.
- [39] J. Kamcev, D. R. Paul, B. D. Freeman, *Macromolecules* **2015**, *48*, 8011.
- [40] R. C. Weast, *Handbook of Chemistry and Physics*, 56th ed., CRC Press, Cleveland, **1975**.
- [41] E. Luyk, *Sputter Coating for SEM: How This Sample Preparation Technique Assists Your Imaging*, <https://www.thermofisher.com/blog/microscopy/sputter-coating-for-sem-how-this-sample-preparation-technique-assists-your-imaging/>, **2019**.
- [42] R. Kiyono, G. H. Koops, M. Wessling, H. Strathmann, *J. Membr. Sci.* **2004**, *231*, 109.
- [43] R. Wycisk, W. M. Trochimczuk, *J. Membr. Sci.* **1992**, *65*, 141.

Manuscript received: April 12, 2022
Revised manuscript received: May 17, 2022
Accepted manuscript online: May 18, 2022

ChemElectroChem

Supporting Information

Determination of Ionic Diffusion Coefficients in Ion-Exchange Membranes: Strong Electrolytes and Sulfates with Dissociation Equilibria

Kuldeep, José A. Manzanares, Pertti Kauranen, Seyedabolfazl Mousaviihashemi, and Lasse Murto \ddot{m} ki*

Calculations of the dissociation constants of sulfate species

1. Sulfuric acid

The concentrations of various ionic species in sulfuric acid were determined by Robertson and Dunford [S1] in a very wide range of concentrations. Here are values in the dilute concentration range.

Table S11. Ionic concentrations in sulfuric acid and the concentration-based dissociation constant, K_c , calculated thereof; m is the molality and c the molar concentration of acid.

m	c (M)	$[H^+]$ (M)	$[SO_4^{2-}]$ (M)	$[HSO_4^-]$ (M)	K_c (M)
0.1	0.099	0.132	0.033	0.066	0.066
0.2	0.198	0.260	0.062	0.136	0.119
0.3	0.296	0.383	0.087	0.210	0.159
0.4	0.393	0.508	0.114	0.279	0.208
0.5	0.490	0.631	0.141	0.349	0.255
0.6	0.586	0.754	0.168	0.418	0.303
0.7	0.681	0.874	0.193	0.488	0.346
0.8	0.775	0.992	0.217	0.558	0.386
0.9	0.869	1.110	0.240	0.620	0.430
1	0.962	1.240	0.280	0.680	0.511

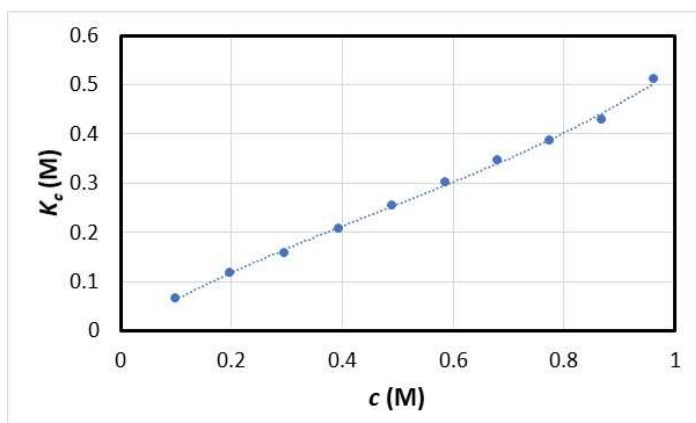


Figure S11. Concentration-based dissociation constant of the bisulfate-sulfate equilibrium.

$$K_c = \frac{[\text{H}^+][\text{SO}_4^{2-}]}{[\text{HSO}_4^-]} \quad (1)$$

A 3rd order interpolation polynomial (dotted curve) was fitted to the data to calculate K_c in intermediate concentrations.

2. Sodium sulphate

A freeware VisualMinteq[®] software [S12] was applied to calculate the ionic equilibria of Na_2SO_4 . The results are collected in Table S12.

Table S12. Ionic activities and concentrations in Na_2SO_4 solutions, along with the thermodynamic dissociation constant, K_a , and the concentration-based dissociation constant, K_c .

$[\text{Na}_2\text{SO}_4]$ (M)	$[\text{Na}^+]$ (M)	$[\text{SO}_4^{2-}]$ (M)	$[\text{NaSO}_4^-]$ (M)	Na^+ activity	SO_4^{2-} activity	NaSO_4^- activity	K_a	K_c (M)
0.0100	0.0195	0.0095	0.0005	0.0166	0.0050	0.0005	0.182	0.347
0.0500	0.0931	0.0431	0.0100	0.0695	0.0137	0.0100	0.182	0.578
0.1000	0.1809	0.0809	0.0191	0.1258	0.0197	0.0136	0.182	0.764
0.2500	0.4327	0.1827	0.0673	0.2693	0.0297	0.0440	0.182	1.176

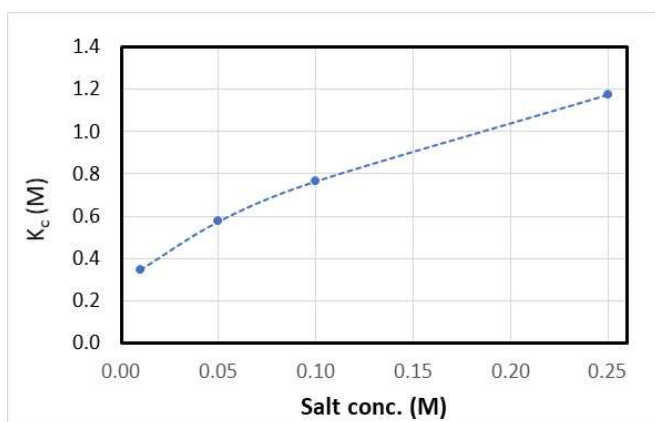


Figure S12. Concentration-based dissociation constant of the NaSO_4^- -sulfate equilibrium.

41
$$K_c = \frac{[\text{Na}^+][\text{SO}_4^{2-}]}{[\text{NaSO}_4^-]} \quad (2)$$

42 A power interpolation function (dashed curve) was fitted to the data to calculate K_c in intermediate
43 concentrations.

44

45 SI1. E.B. Robertson, H.B. Dunford, *J. Am. Chem. Soc.* **1964**, *86*, 5080.

46 SI2. <https://vminteq.lwr.kth.se/>

47